

University of Warwick institutional repository: <http://go.warwick.ac.uk/wrap>

This paper is made available online in accordance with publisher policies. Please scroll down to view the document itself. Please refer to the repository record for this item and our policy information available from the repository home page for further information.

To see the final version of this paper please visit the publisher's website. Access to the published version may require a subscription.

Author(s): T. E. Whall, A. D. Plews, N. L. Matthey, P. J. Phillips and U. Ekenberg

Article Title: Effective mass and band nonparabolicity in remote doped Si/Si_{0.8}Ge_{0.2} quantum wells

Year of publication: 1995

Link to published version: <http://dx.doi.org/10.1063/1.113501>

Publisher statement: none

Effective mass and band nonparabolicity in remote doped Si/Si_{0.8}Ge_{0.2} quantum wells

T. E. Whall, A. D. Plews,^{a)} N. L. Matthey, and P. J. Phillips
Department of Physics, University of Warwick, Coventry CV4 7AL, United Kingdom

U. Ekenberg
Department of Physics, Royal Institute of Technology, 10044 Stockholm, Sweden

(Received 19 December 1994; accepted for publication 28 February 1995)

The effective masses in remote doped Si/Si_{0.8}Ge_{0.2}/Si quantum wells having sheet densities, N_s in the range $2 \times 10^{11} - 1.1 \times 10^{12} \text{ cm}^{-2}$ have been determined from the temperature dependencies of the Shubnikov–de Haas oscillations. The values obtained increase with magnetic field and N_s . This behavior is taken as evidence for the nonparabolicity of the valence band and accounts for the discrepancies in previously reported masses. Self-consistent band structure calculations for a triangular confinement of the carriers have also been carried out and provide confirmation of the increase in mass with N_s . Theory and experiment give extrapolated Γ point effective masses of 0.21 and 0.20 of the free-electron mass, respectively. © 1995 American Institute of Physics.

We recently reported the dependence of the hole effective mass, m^* on Ge concentration x , in molecular beam epitaxy (MBE) grown remote doped Si/Si_{1-x}Ge_x quantum wells with $0.05 < x < 0.3$.¹ The measured masses clearly showed the effects of the strain inherent to this system but, in common with measurements reported by other workers,²⁻⁵ were somewhat higher than the Γ point values obtained from band structure calculations.^{6,7} The lowest value of m^* measured in a Si_{1-x}Ge_x channel is $(0.23 \pm 0.03) m_0$, obtained for $x=0.13$, with $n_s = 2 \times 10^{11} \text{ cm}^{-2}$.^{1,8} There remains some controversy over whether the observed values of m^* follow the predicted dependence of strain (i.e., Ge content). In particular Cheng *et al.*² report m^* decreasing with increasing x (as predicted) while Kiehl *et al.*³ observe no dependence on x which they attribute to compositional nonuniformity. Also, the band structure calculations have been carried out either for the bulk alloy⁶ or have included a square well confinement,⁷ rather than the triangular confinement resulting from doping one side of the quantum well as usually measured.

Previously, we demonstrated that our results were consistent with the predicted behavior and suggested that the reported discrepancies may be due to the valence band nonparabolicity in view of the fact that the measured samples were of a wide range of carrier sheet density ($10^{11} - 10^{13} \text{ cm}^{-2}$).¹ To provide evidence for the nonparabolicity we have investigated the dependence of the measured m^* on magnetic field and on carrier sheet density. The results are compared with calculations carried out in the envelope function approximation taking into account the approximately triangular form of the quantum well and including heavy-hole, light-hole, and spin-split subbands.

A set of samples was grown by solid source MBE, each consisting of a 300 nm undoped Si buffer on an n -(100) substrate followed by a 30 nm alloy layer, an undoped Si spacer layer and a 50 nm B doped cap. A self-consistent

model⁹ was used to design the structures to give sheet densities, N_s in the range $10^{11} - 10^{12} \text{ cm}^{-2}$. To achieve the upper limit of N_s , $x=0.20$ was chosen. Table I shows the resulting spacer layer thicknesses along with the corresponding sheet carrier densities obtained from the period of the Shubnikov–de Haas oscillations in $1/B$ and the Hall mobility at a temperature of 4 K. Double crystal x-ray diffraction was used to confirm that the layers were fully strained. Magnetotransport measurements were carried out on Hall bars fabricated using photolithography/wet etching.

To determine m^* we follow our previously reported analysis of the temperature dependence of the Shubnikov–de Haas oscillation,^{1,8} which accounts for the effects of temperature dependent screening, weak localization, and hole-hole interactions. The effective mass is used as an adjustable parameter to obtain unity gradient in a plot of $\ln[\Delta\rho_m(T)/\rho_0(T)]$ versus $\{\ln(\xi/\sinh \xi) - [\pi/\omega_c\tau_q(T)]\}$ where $\Delta\rho_m$ is the peak value of the longitudinal resistivity extracted using a cubic spline interpolation and rectangular digital filter, ρ_0 is the Boltzmann resistance, $\xi = 2\pi^2kT/\hbar\omega_c$, $\omega_c = eB/m^*$, and τ_q is the quantum lifetime. The temperature dependence of the Boltzmann resistivity, ρ_0 is extracted from the measured temperature dependence by fitting the conductance to

$$\sigma_{xx}(T) = [\rho_0(T=0)]^{-1} [1 - \gamma(T/T_F)] - A \ln[kT\tau/\hbar], \quad (1)$$

where γ is a screening parameter ~ 1 for interface roughness and interface charge scattering which are expected to domi-

TABLE I. Spacer layer thickness L_s , sheet carrier density N_s and 4 K Hall mobility, μ for the samples under investigation

L_s/nm	$N_s/10^{11} \text{ cm}^{-2}$	$\mu/\text{cm}^2 \text{ V}^{-1} \text{ s}^{-1} @ 4 \text{ K}$
45	2.0	2750
20	4.0	2960
10	4.8	2850
4	7.7	2300
2	10.5	1440

^{a)}Present address: Department of Electrical and Electronic Engineering, University of Leeds, Leeds LS2 9JT, UK.

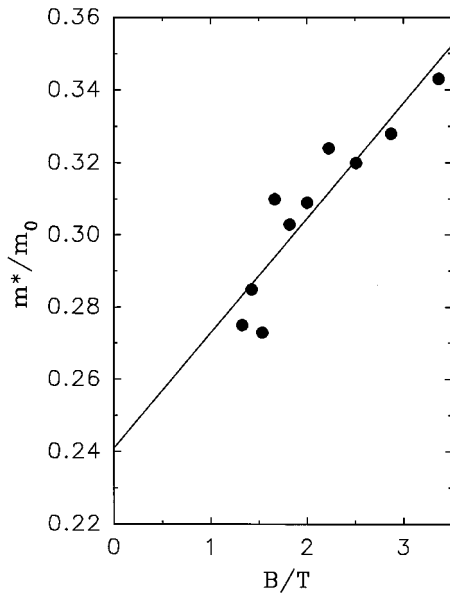


FIG. 1. Dependence of measured effective mass, m^* on magnetic field, B for a sample of sheet carrier density $4.8 \times 10^{11} \text{ cm}^{-2}$.

nate in these samples^{9,10} and A is a measure of weak localization and hole-hole interaction effects. $\tau_q(T)$ is then obtained by assuming $\tau_q \approx \tau$ the transport lifetime—a reasonable approximation for short range scattering.

In contrast to our previous work (largely with samples of lower strain and sheet density) we observe a significant magnetic field dependence of m^* as illustrated in Fig. 1. In all cases we observe m^* increasing with B . This is a consequence of the nonparabolicity of the subband: an increasing B corresponds to larger values of the wave vector in the plane of the 2D hole gas, k_{\parallel} and increasing flattening of the $E(k)$ curve of the lowest subband because of the interaction with higher subbands. Here, we assume states below the valence band edge have positive energies, as is the convention for holes. To provide a meaningful comparison between samples we take the extrapolated zero magnetic field values of m^* since the cyclotron mass tends to the classical value as B tends to zero.^{11,12} Figure 2 shows these extrapolated values of m^* (solid circles) and the mean value of m^* (open circles) plotted as a function of the carrier sheet density obtained from the period of the Shubnikov–de Haas oscillations in $1/B$.

The experimental values are compared with the results of self-consistent calculations in the envelope function approximation (shown in Fig. 2 as solid squares). A multiband theory including the heavy-hole, light-hole, and spin-orbit-split bands and incorporating the matrix given in Ref. 13 was used with the intended growth parameters and assuming a B doping concentration of $3 \times 10^{18} \text{ cm}^{-3}$ and a background impurity concentration of 10^{15} cm^{-3} n -type. The masses at the Fermi wave vector k_F and at $k_{\parallel}=0$ were determined numerically from the curvature of the lowest subband with an accuracy estimated to be of the order $0.01m_0$. As can be seen in Fig. 2 the theoretical values of $m^*(k_F)$ are somewhat smaller than the experimental ones, although with the exception of the highest sheet density, the theoretical values lie

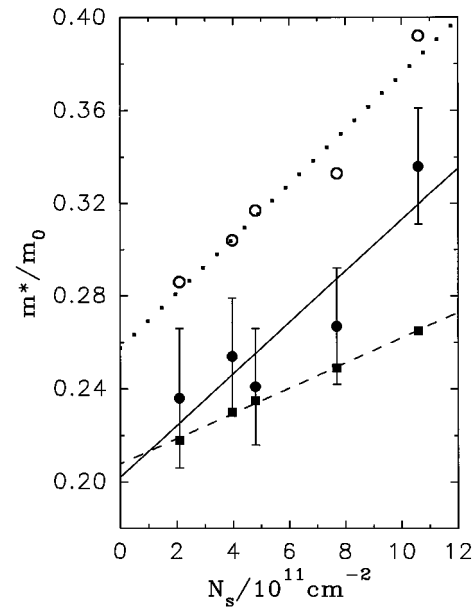


FIG. 2. Effective mass, m^* , plotted as a function of sheet carrier density, N_s . Open circles: mean values of m^* for $1 < B < 6\text{T}$, solid circles: $B=0$ values of m^* , solid squares: calculated values of m^* . The solid line represents a linear extrapolation of the $B=0$ experimental data to $N_s=0$, the dashed line is a linear fit through the calculated data and the dotted line is an extrapolation of the mean experimental masses.

within the estimated experimental uncertainty. In addition the increase of m^* with N_s is well reproduced. A linear extrapolation of the zero magnetic field data to $N_s=0$ gives $m^*(k=0) \cong 0.20m_0$ as compared to a value of $m^*(k=0) \cong 0.21m_0$ from theory.

These masses are remarkably close to the ideal limit for decoupled bands. From inspection of the Hamiltonian¹³ it is found that the mass approaches $(\gamma_1 + \gamma_2)^{-1}$ in the limit that the interaction between subbands tends to zero. For the Luttinger parameters γ_1 and γ_2 which are deduced as discussed later for $\text{Si}_{0.8}\text{Ge}_{0.2}$, this ideal mass is $0.187m_0$. The fact that the masses in this system are close to this value is largely due to the compressive strain in the quantum well which increases the energy of the light-hole band edge relative to the heavy-hole band edge and decreases the interaction between light-hole and heavy-hole subbands. In the present case this effect is enhanced by the doping profile which results in a spatial separation of heavy and light holes (Ref. 14). The light-hole potential is found to be lower in the Si beyond the spacer layer than in the quantum well, whereas the opposite situation applies for heavy holes.

In the asymmetric, roughly triangular potential resulting from doping only one side of the quantum well, a spin splitting of the subbands for $k_{\parallel} \neq 0$ is expected.^{11,12} This is due to the interaction of the built-in-electric field and spin-orbit coupling. In the present case, the spin splitting is found to be fairly small and the difference in mass between the two spin states is not expected to be seen in these experiments. The theoretical masses shown in Fig. 2 are an average of these two masses.

The dependence of the calculated masses on variations in growth parameters has been investigated since parameters

such as B doping concentration and spacer layer thickness have uncertainties of the order 10% and the background impurity concentration is not well known. Plausible variations of these parameters do not seem to account for the discrepancy between theory and experiment for the sample with $N_s = 1.1 \times 10^{12} \text{ cm}^{-2}$, but are sufficient to account for the discrepancies in the remaining data. We have shown that interface charge is present in our material with sheet densities in the range $10^{10} - 10^{11} \text{ cm}^{-2}$,^{9,10} this has not been included in the present calculations but is thought unlikely to have a significant effect on the masses or to explain the discrepancy at high sheet density where one would expect its effect to be smallest. Another source of uncertainty is the calculation of the important Luttinger parameters for $\text{Si}_{0.8}\text{Ge}_{0.2}$. We have used linear interpolation between Si and Ge of the heavy-hole mass along (100) and (111) and the light-hole mass along (100) and deduced the Luttinger parameters from this.

According to theory, the nonparabolicity may be described by $\hbar^2 k^2 / 2m_{k=0}^* = \epsilon [1 + c\epsilon/\Delta]$ where c is a nonparabolicity factor and Δ is the heavy-light hole splitting.^{15,16} A linear dependence is predicted over this range of N_s , and using the theoretical band edge effective mass for this Ge concentration, we obtain an average nonparabolicity factor of $c=0.4$, in reasonable agreement with the value of 0.5 deduced for samples with varying Ge content.¹

Our analysis makes the assumption that the transport and quantum lifetimes are equal, this being true only for short range scattering. It is possible to extract τ/τ_q from a Dingle plot of $\ln[(\Delta\rho_m \sinh \xi)/\rho_0 \xi]$ versus $1/B$ since the gradient may be written as $-\pi\tau/\tau_q\mu_0$. We obtain an average value of $\tau/\tau_q = 1.0 \pm 0.2$ which is consistent with our previous work where we demonstrated that interface charge and interface roughness scattering are dominant in the present samples.^{9,10}

In conclusion, we have measured the hole effective mass as a function of the magnetic field and carrier sheet density in remote doped quantum wells in $\text{Si}/\text{Si}_{0.8}\text{Ge}_{0.2}$. We find from

both theory and experiment that m^* increases with N_s , which, along with the increase of the measured m^* with magnetic field, is taken as evidence of the valence band nonparabolicity. However, further work is needed to discover the source of the discrepancy between the theoretical and experimental values of m^* at the highest N_s . A linear extrapolation of the measured data gives $m_{(k=0)}^* \cong 0.20m_0$, which is in satisfactory agreement with the predicted band edge value of $0.21m_0$. An average nonparabolicity factor of 0.4 is obtained in reasonable agreement with our previous work.

The authors have enjoyed useful discussions with Dr. Robin Nicholas.

- ¹T. E. Whall, A. D. Plews, N. L. Matthey, and E. H. C. Parker, *Appl. Phys. Lett.* **65**, 3362 (1994).
- ²J. P. Cheng, V. P. Kesan, D. A. Grutzmacher, and T. O. Sedgewick, *Appl. Phys. Lett.* **64**, 1681 (1994).
- ³R. A. Kiehl, P. E. Batson, J. O. Chu, D. C. Edelstein, F. F. Fang, B. Laikhtman, D. R. Lombardi, W. T. Masselink, B. S. Meyerson, J. J. Nocera, A. H. Parsons, C. L. Stanis, and J. C. Tsang, *Phys. Rev. B* **48**, 11946 (1993).
- ⁴F. F. Fang, P. J. Wang, B. S. Meyerson, J. J. Nocera, and K. E. Ismail, *Surf. Sci.* **263**, 175 (1992).
- ⁵R. People, J. C. Bean, and D. V. Lang, *J. Vac. Sci. Technol. A* **3**, 846 (1985).
- ⁶S. R. Chun and K. L. Wang, *IEEE Trans. Electron Devices* **ED-39**, 2153 (1993).
- ⁷B. Laikhtman and R. A. Kiehl, *Phys. Rev. B* **47**, 10515 (1993).
- ⁸T. E. Whall, N. L. Matthey, A. D. Plews, P. J. Phillips, O. A. Mironov, R. J. Nicholas, and M. J. Kearney, *Appl. Phys. Lett.* **64**, 357 (1994).
- ⁹C. J. Emeleus, T. E. Whall, D. W. Smith, R. A. Kubiak, E. H. C. Parker, and M. J. Kearney, *J. Appl. Phys.* **73**, 3852 (1993).
- ¹⁰E. Basaran, R. A. Kubiak, T. E. Whall, and E. H. C. Parker, *Appl. Phys. Lett.* **64**, 3470 (1994).
- ¹¹U. Ekenberg and M. Altarelli, *Phys. Rev. B* **32**, 3712 (1985).
- ¹²J. P. Eisenstein, H. L. Stormer, V. Narayanamurti, A. C. Gossard, and W. Wiegmann, *Phys. Rev. Lett.* **53**, 2579 (1984).
- ¹³U. Ekenberg, W. Batty, and E. P. O'Reilly, *J. Phys. Colloq. C* **5**, 553 (1987).
- ¹⁴A. Ghiti and U. Ekenberg, *Semicond. Sci. Technol.* **9**, 1575 (1994).
- ¹⁵G. C. Osborne, J. E. Schirber, T. J. Drummond, L. R. Dawson, B. L. Doyle, and I. J. Fritz, *Appl. Phys. Lett.* **49**, 731 (1986).
- ¹⁶B. A. Foreman, *Phys. Rev. B* **49**, 1757 (1994).